Mode conversion in quadratic nonlinear crystals

Tal Ellenbogen,* Ido Dolev, and Ady Arie

Department of Physical Electronics, Faculty of Engineering, Tel-Aviv University, Tel-Aviv 69978, Israel
**Corresponding author: ellenbog@post.tau.ac.il*

Received March 12, 2008; accepted March 30, 2008;
posted April 24, 2008 (Doc. ID 93679); published May 27, 2008

We propose a novel all-optical, nonlinear mode-conversion scheme based on cascaded three-wave-mixing phase-matched interactions in quadratic nonlinear crystals. We demonstrate the method experimentally by performing all-optical mode conversion of an input 1636 nm Hermite–Gaussian mode from the zeroth order to the first order using two periodically poled $LiNbO_3$ crystals. Nonlinear mode conversion of an input beam into a higher order, orthogonally polarized output beam can be realized using only one quasiperiodic nonlinear structure. Moreover, it can be enhanced for conversion of complex modes, e.g., Laguerre–Gaussian or Bessel modes. © 2008 Optical Society of America

OCIS codes: 190.2620, 190.4223, 140.3300, 190.4360.

In recent years, there has been increasing interest in spatial beam shaping, i.e., creating laser beams with particular transverse phase and intensity distributions. Some applications require generation of pure high-order modes, e.g., atom manipulations [1], photon entanglement experiments [2], and unique optical imaging techniques [3], while other applications require "ideal" Gaussian beams that have the smallest divergence angle and can be focused to a minimal spot size. Various methods have been developed recently for intracavity mode selection [4] or extracavity mode conversion [5] using linear diffractive elements. In this work we suggest and experimentally demonstrate, for the first time to our knowledge, a new method for all-optical nonlinear mode conversion, while maintaining the initial beam frequency. The nonlinear mode conversion scheme is based on cascaded three wave mixing processes that can be controlled in an all-optical manner and tuned to convert beams at different wavelengths using the same device.

For sum frequency generation (SFG), the spatial dependency of the local oscillating electric field at $z=z_0$ created by the oscillating polarization in a quadratic crystal slab of length δz is $\delta E_c(x,y,z_0) = \kappa E_b(x,y,z_0) E_a(x,y,z_0)\delta z$, where $E_{a,b}$ are the spatial dependencies of the generating waves, z is the propagation direction, and κ is the nonlinear coupling coefficient. It was recently shown that the spatial distribution of laser beams can be transferred in three wave mixing processes between the interacting waves [6,7] or between an engineered nonlinear photonic structure and the optical waves [8]. For demonstration of this concept we can consider waves propagating in the z direction, which are plane waves in the y direction and Hermite–Gaussian (HG) modes in the x direction. The spatial distribution of such waves is

$$U_m(x,z) = A_m \frac{W_0}{W(z)} G_m\left[\frac{\sqrt{2}x}{W(z)}\right] \exp\left[-ikz - ik\frac{x^2}{2R(z)} + i(m+1)\xi(z)\right], \quad (1)$$

where A_m is the amplitude and W_0 and $W(z)$ are the waist and local beam radii, respectively, $G_m(u)$ is the mth order Hermite Gaussian function, k is the wave vector, $R(z)$ is the curvature, and ξ is the Gouy phase. If we consider the SFGs of HG_0 and HG_1 taking into account Eq. (1) and the relation $G_0(W_a)G_1(W_b)=A\cdot G_1(W_c)$, the local spatial pattern of the oscillating electric field is

$$\delta E_c(x,z_0) = A(z_0) G_1\left[\frac{\sqrt{2}x}{W(z_0)}\right] \exp\left[-i(k_a+k_b)z_0 - i\left(\frac{k_a}{2R_a(z_0)} + \frac{k_b}{2R_b(z_0)}\right)x^2 + 2i\xi(z_0)\right]\delta z, \quad (2)$$

where $A(z_0)$ is the amplitude of the generated oscillating electric field. Equation (2) demonstrates that the local transverse pattern of the generated electric field is in the form of HG_1 distribution. The coherent addition of the radiation generated by all the local oscillations along the crystal is determined by the phase matching conditions of the interacting waves.

The total generated radiation can be calculated using a split-step Fourier numerical simulation [9]. Figure 1 shows the simulated far field phase and inten-

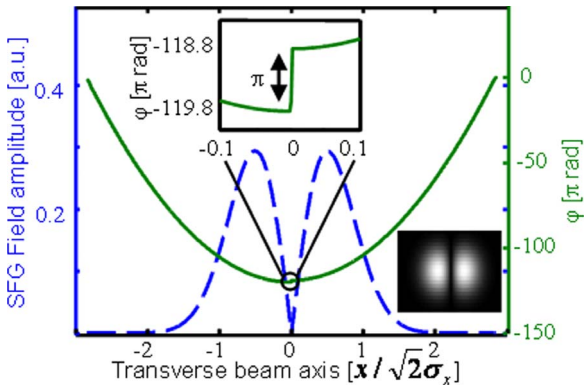

Fig. 1. (Color online) Numerical results for amplitude (dashed curve) and phase profiles (solid curve) of far field outputs for sum frequency of HG_0+HG_1. The top inset shows π phase singularity, and the right-hand-side inset shows 2D intensity intersection of the output beam.

sity distribution of the radiation at 638 nm wavelength, which is the output of SFG process of HG_0 (1636 nm) and HG_1 (1047 nm) generated from a 1 cm long crystal. The interaction is quasi-phase-matched using a periodically poled $LiNbO_3$ crystal with a period of 11.75 μm and generates output radiation with transverse distribution, which is similar to that of an ideal HG_1 mode. Calculating the M^2 quality factor for the generated beam results in $M^2=3$, which is the theoretical value for a pure HG_1 mode [10]. The simulation shows similar results for the phase and intensity distributions of an electric field at 1636 nm, which is the output of a difference frequency generation (DFG) process of HG_1 (638 nm) and HG_0 (1047 nm). These two processes, i.e., SFG and DFG, can be cascaded to perform all-optical nonlinear mode conversion at the same wavelength.

The nonlinear mode-conversion scheme proposed here is shown in Fig. 2(a). To convert an arbitrary wave from HG_0 to HG_1, a pump laser beam at the two modes should be used. First, the HG_1 pump beam is mixed with the signal in a SFG process to get a HG_1 mode at the sum of frequencies, then the generated HG_1 mode is mixed with the HG_0 pump beam in a DFG process to get the desired HG_1 mode at the original signal frequency. Both processes should be phase matched for efficient interactions. It is very important to note that the longitudinal phase matching by birefringence or by periodically poled quasi-phase-matching (QPM) structures is not always sufficient to compensate the spatial decoherence of the generated waves and does not always allow the buildup of a pure mode at the output. This fact is demonstrated in Figs. 2(b) and 2(c) that show M^2 values of the output beams for the SFG and DFG processes for the same waves as shown in Fig. 1 with respect to different waist radiuses of the generating waves. It is shown that there are interactions where the M^2 value of the resulting output beam deviates from $M^2=3$, therefore indicating that the mode is not a pure HG_1 mode. Nevertheless, by choosing the proper beam parameters, an ideal mode transfer can be achieved. We have used this fact in a cascaded nonlinear process to experimentally achieve all-optical nonlinear mode conversion of a 1636 nm HG_0 input beam to a HG_1 output beam at the same wavelength.

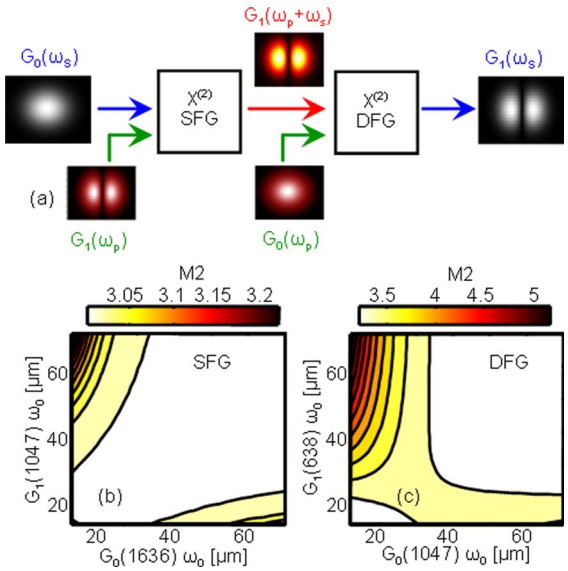

Fig. 2. (Color online) (a) Nonlinear mode-conversion scheme. (b), (c) Numerical results for beam quality factor M^2 for interactions of beams with different waists for the SFG and DFG processes, respectively ($M^2=3$ is the theoretical value for an ideal HG_1 beam).

The experimental setup for nonlinear mode conversion is illustrated in Fig. 3. A Q-switched Nd:YLF source with a repetition rate of 2 kHz and pulse width of ~7.2 ns was split to three beams. One was transformed to an approximated HG_1 mode using a binary phase plate and was used as the pump for the SFG stage of nonlinear conversion. Another beam was used as the HG_0 pump beam for the DFG stage of the nonlinear mode conversion, and the third beam was used to pump an optical parametric oscillator (OPO) device that was thermally tuned to generate signal radiation at 1636 nm at an approximated HG_0 mode. The OPO output was used as the signal beam in the experiment. Phase matching at the first SFG and second DFG stages was performed by two periodically poled $LiNbO_3$ crystals with 11.75 μm periods. The crystals were placed on temperature controlled stages that were set to the phase matching point of $T=124°C$. To filter the 1636 and 1047 nm waves after the first stage, a high-pass filter was used that consisted of six visible mirrors with reflectivity below 10% for wavelengths above 700 nm and a near IR mirror to filter the remaining Nd:YLF wave. Far field images for the 1047 and 1636 nm beams were taken by a MicronViewer 7290 camera, and the 638 nm far field image was taken by a Cannon digital camera. Intensities were measured by Ophir visible, IR, and thermal detectors.

Nonlinear mode conversion of the input beam was observed. Figures 4(a) and 4(f) show far field images of the input signal HG_0 beam and the converted output signal HG_1 beam. Figures 4(b) and 4(e) show far field images of the HG_0 and HG_1 pump beams, respectively, and Fig. 4(c) shows the 638 nm HG_1 output of the SFG process. The average power of the participating beams was 4.2 mW (400 nW), 4.5 mW (6.15 mW), and 180 μW (80 μW) for 1636, 1047, and 638 nm, respectively, at the SFG (DFG) stages of the experiment. The internal efficiencies of the SFG and DFG processes were 0.021 and 0.0019 $\%W^{-1}$, respectively, considering the Fresnel reflection from both surfaces of the uncoated crystal. As expected, the dependence of the efficiency of output beams on the

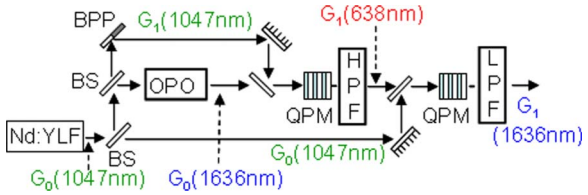

Fig. 3. (Color online) Experimental setup for nonlinear mode conversion of the OPO signal output HG_0 (1636 nm) into HG_1 (1636 nm). BS, beam splitter; BPP, binary phase plate; HPF, high-pass filter; and LPF, low-pass filter.

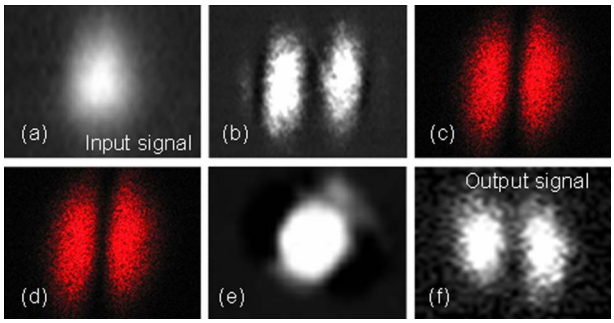

Fig. 4. (Color online) Far field photos of participating beams: (a) and (f) HG_0 signal input and HG_1 converted signal output at 1636 nm, (b) pump HG_1 (1047 nm) for the SFG process, (c) output HG_1 (638 nm) of the SFG process, (d) signal input to the DFG process HG_1 (638 nm), and (e) pump HG_0 (1047 nm) input to the DFG process.

power of each of the input beams was measured to be linear at both the SFG and DFG processes. The calculated internal efficiencies were 0.98 and 0.12 $\%W^{-1}$ for the SFG and DFG processes, respectively. The one and one-half orders of magnitude differences between experimental efficiency and numerical calculations result from structural defects in the QPM structure, deviations of the duty cycle from a perfect 50%, experimental deviations from a collinear QPM interaction, and deviations from a perfect spatial overlap of the generating beams.

The M^2 values of a diverging beam can be calculated using the next general divergence relation $W_x^2(z) = W_{0x}^2 + (M_x^2)^2(\lambda/\pi W_{0x})^2(z-z_0)^2$, where W_x is twice the standard deviation (σ_x), which is calculated from the second moment of the transverse distribution; z_0 and W_{0x} are the waist location and size, respectively; and λ is the wavelength. The transverse profiles of the beams in the experiment were measured by knife edge at the waist and far field, and the measurements were used to estimate the M^2 values of the beams. $2\sigma_x$ values were estimated by fitting best HG_1 or HG_0 to the measured knife-edge profiles and calculating the second moment of the fitted curve. In addition, $2\sigma_x$ values were estimated by 20%–80% knife-edge values for HG_1 distribution and 16%–84% knife-edge values for HG_0 distribution. We have used both approaches for estimation because of low knife-edge resolution at the beam waists. The M^2 values of the input and output 1636 nm beams were 1.46 ± 0.35 and 2.54 ± 0.25, respectively. The rest of the measured M^2 values were 3.05 ± 0.13, 3.05 ± 0.15, and 1.85 ± 0.25 for the HG_1 (1047 nm), HG_1 (638 nm), and HG_0 (1047 nm), respectively. The differences between experimental M^2 measurements and ideal values result from rotation of the beams with respect to the knife edge that is decreasing M^2 values for HG_1 beams and increasing M^2 values for HG_0 beams because of their ellipticity. In addition, the high M^2 value for HG_0 (1047 nm) results from low beam quality.

To get a pure HG_1 mode at the output of the nonlinear conversion scheme we have used two crystals and divided the experimental setup into two stages. After the first stage of SFG we filtered out the signal wave at the original mode, and in the second stage of DFG the signal wave at the new mode was generated. However, the nonlinear mode-conversion scheme can be realized using only a single quasiperiodic structure [11], where the generated HG_1 beam is orthogonally polarized with respect to the input HG_0 beam; thus the two beams can be separated by a polarizing beam splitter. For crystals from the trigonal $3m$ symmetry group, ordinary polarized HG_1 pump and HG_0 signal waves can be upconverted to an extraordinary polarized idler wave (using the d_{eoo} element of the nonlinear tensor), followed by downconversion of this idler wave with an extraordinary polarized HG_0 pump to yield an extraordinary polarized HG_1 signal wave (using the d_{eee} element).

In conclusion, we have suggested and experimentally demonstrated a nonlinear mode-conversion scheme. By enabling two cascaded three wave mixing processes, we could convert a HG_0 laser mode to a HG_1 mode at the same frequency with experimental results that agree well with numerical calculations. The nonlinear mode-conversion scheme can be realized using two birefringent or QPM crystals or using only one quasiperiodic structure. The advantages of nonlinear mode conversion are that it can be tuned by changing phase matching conditions, e.g., temperature or QPM periods, to fit different wavelengths using the same pump and can be all-optically controlled. Moreover, it can be enhanced for conversion to modes other than HG_1, e.g., higher-order HG modes, Laguerre–Gaussian modes, and Bessel beams, and can be combined with nonlinear temporal shaping of the beams.

The authors thank N. Davidson for the binary phase plate. This work was supported by the Israel Science Foundation, grant 960/05, and by the Israeli Ministry of Science, Culture, and Sport.

References

1. T. Kuga, Y. Torii, N. Shiokawa, T. Hirano, Y. Shimizu, and H. Sasada, Phys. Rev. Lett. **78**, 4713 (1997).
2. A. Mair, A. Vaziri, G. Weihs, and A. Zeilinger, Nature **412**, 313 (2001).
3. L. Novotny, E. J. Sánchez, and X. S. Xie, Ultramicroscopy **71**, 21 (1998).
4. A. Ishaaya, N. Davidson, and A. Friesem, Opt. Express **13**, 4952 (2005).
5. J. Courtial and M. J. Padgett, Opt. Commun. **159**, 13 (1999).
6. P. H. Souto Ribeiro, D. P. Caetano, M. P. Almeida, J. A. Huguenin, B. Coutinho dos Santos, and A. Z. Khoury, Phys. Rev. Lett. **87**, 133602 (2001).
7. K. Dholakia, N. B. Simpson, M. J. Padgett, and L. Allen, Phys. Rev. A **54**, 3742 (1996).
8. A. Bahabad and A. Arie, Opt. Express **15**, 17619 (2007).
9. T. Ellenbogen, A. Arie, and S. M. Saltiel, Opt. Lett. **32**, 262 (2007).
10. S. Saghafi and C. J. R. Sheppard, Opt. Commun. **153**, 207 (1998).
11. K. Fradkin-Kashi, A. Arie, P. Urenski, and G. Rosenman, Phys. Rev. Lett. **88**, 023903 (2002).